Manifestations of impurity-induced $s_{\pm} \Rightarrow s_{++}$ transition: multiband model for dynamical response functions

2013 New J. Phys. 15 013002

(http://iopscience.iop.org/1367-2630/15/1/013002)

New Journal of Physics
The open access journal for physics

Manifestations of impurity-induced $s_{\pm} \Rightarrow s_{++}$ transition: multiband model for dynamical response functions

D V Efremov[1,2,5], **A A Golubov**[3] **and O V Dolgov**[1,4]

[1] Max-Planck-Institut für Festkörperforschung, D-70569 Stuttgart, Germany
[2] IFW Dresden, Helmholtzstrasse 20, D-01069 Dresden, Germany
[3] Faculty of Science and Technology and MESA+ Institute of Nanotechnology, University of Twente, 7500-AE Enschede, The Netherlands
[4] P N Lebedev Physical Institute of RAS, Moscow, Russia
E-mail: d.efremov@ifw-dresden.de

New Journal of Physics **15** (2013) 013002 (14pp)
Received 9 September 2012
Published 3 January 2013
Online at http://www.njp.org/
doi:10.1088/1367-2630/15/1/013002

Abstract. We investigate the effects of disorder on the density of states, the single-particle response function and optical conductivity in multiband superconductors with $s_{\pm}$ symmetry of the order parameter, where $s_{\pm} \rightarrow s_{++}$ transition may take place. In the vicinity of the transition, the superconductive gapless regime is realized. It manifests itself in anomalies in the above-mentioned properties. As a result, intrinsically phase-insensitive experimental methods such as angle-resolved photoemission spectroscopy, tunneling and terahertz spectroscopy may be used to reveal information about the underlying order parameter symmetry.

[5] Author to whom any correspondence should be addressed.

Contents

1. Introduction

The discovery of iron-based superconductors (FeSC) [1] resulted in experimental and theoretical efforts at understanding the reason for the rather high critical temperatures and symmetry of superconducting order parameters in these compounds. These studies yielded a comprehensive experimental description of the electronic Fermi surface structure, which includes multiple Fermi surface sheets in good agreement with density functional calculations [2]. The Fermi surface of the moderate doped FeSC is given by two hole pockets around the $\Gamma = (0, 0)$ point and two electron pockets around the $M = (\pi, \pi)$ point in the folded zone. This band structure suggests strong antiferromagnetic fluctuations, which may be a mechanism for electron pairing. In this case, the natural order parameter for most of the FeSC is the so-called $s_{\pm}$ state, described by the order parameter $\tilde{\phi}$ (see the definition below) with different signs for electron- and hole-like pockets [3].

This model agrees well with the nodeless character of the order parameter experimentally found for most of the moderately doped FeSC [4–7]. However, the question of whether the order parameter $\tilde{\phi}$ at low frequencies changes its sign by changeover from electron-like to hole-like pockets is still under discussion. Moreover, the relative robustness of the superconductors against nonmagnetic impurities led to a suggestion that a more conventional two-band order parameter with the same sign on all Fermi pockets (s_{++}) is realized in these systems [8].

In our previous paper [9] it was demonstrated that not only superconductors with s_{++} order parameter but also $s_{\pm}$ may be robust against nonmagnetic impurities. Therefore, the robustness against nonmagnetic impurities cannot be considered as a strong argument against $s_{\pm}$ order parameter. Moreover, it was shown that there are two types of $s_{\pm}$-superconductors with respect to disorder [9, 10]. In the first one, T_c goes down with an increase of disorder, until it vanishes at a critical value of the scattering rate. This behavior is similar to the famous case of the Abrikosov–Gor'kov magnetic impurities which is widely discussed in the literature. In the second type of $s_{\pm}$ superconductors, T_c tends to a finite value as disorder increases [10]; at the same time the order parameters for the electron-like and hole-like Fermi surfaces acquire the same signs, i.e. the transition from $s_{\pm}$ to s_{++} state occurs. In the dirty limit the gap functions

converge to the same value [11]. We would like to note that the $s_{\pm} \to s_{++}$ transition occurs at a certain critical scattering rate at any temperature including $T = 0$.[6]

In this paper we discuss how the disorder-induced transition $s_{\pm} \to s_{++}$ can manifest itself in single-particle properties and optical conductivity. We show that the disorder dependence of these characteristics at the transition point is a strongly nonmonotonic function of the impurity scattering rate and can be observed in tunneling spectroscopy, angle-resolved photoemission spectroscopy (ARPES) and optics. Therefore, a systematic study of disorder effects using the above-mentioned phase insensitive techniques may provide information about the underlying order parameter symmetry in the clean limit.

The paper is organized as follows. In section 2 we discuss the model and approximations used for the calculations. Section 3 is devoted to single-particle properties. We discuss how the transition $s_{\pm} \to s_{++}$ manifests itself in ARPES and tunneling spectroscopy. In section 4 we calculate the two-particle response function and discuss peculiarities that can be seen in optical conductivity in the vicinity of the transition point.

2. The formalism

For the calculations, we employ the standard approach of (ξ-integrated) Green functions in the Nambu and band space [13]:

$$\hat{\mathbf{g}}(\omega) = \begin{pmatrix} \mathbf{g}_a & 0 \\ 0 & \mathbf{g}_b \end{pmatrix}, \tag{1}$$

with band quasiclassical Green functions

$$\mathbf{g}_\alpha(\omega) = -\mathrm{i}\pi N_\alpha \frac{\tilde{\omega}_\alpha \hat{\tau}_0 + \tilde{\phi}_\alpha \hat{\tau}_1}{\sqrt{\tilde{\omega}_\alpha^2 - \tilde{\phi}_\alpha^2}}, \tag{2}$$

where the $\hat{\tau}_i$ denote Pauli matrices in the Nambu space and N_α is the density of states (DOS) on the Fermi level in the band $\alpha = a, b$ (for the sake of simplicity the two-band model is considered). Here the order parameter $\tilde{\phi}_\alpha = \tilde{\phi}_\alpha(\omega)$ and the renormalized frequency $\tilde{\omega}_\alpha = \tilde{\omega}_\alpha(\omega)$ are complex functions.

The function $\hat{\mathbf{g}}_\alpha$ is related to the full Green function

$$\hat{\mathbf{G}}_\alpha(\mathbf{k}, \omega) = \frac{\tilde{\omega}_\alpha \hat{\tau}_0 + \xi_\alpha(\mathbf{k})\hat{\tau}_3 + \tilde{\phi}_\alpha \hat{\tau}_1}{\tilde{\omega}_\alpha^2 - \xi_\alpha^2(\mathbf{k}) - \tilde{\phi}_\alpha^2} \tag{3}$$

by the standard procedure of ξ-integration $\hat{\mathbf{g}}_\alpha(\omega) = N_\alpha \int \mathrm{d}\xi_\alpha(\mathbf{k}) \hat{G}_\alpha(\mathbf{k}, \omega)$.

The quasiclassical Green functions are obtained by numerical solution of the Eliashberg equations [13–17]:

$$\tilde{\omega}_\alpha(\omega) - \omega = \sum_{\beta=a,b} \left\{ \int_{-\infty}^{\infty} \mathrm{d}z K_{\alpha\beta}^{\tilde{\omega}}(z, \omega) \mathrm{Re} \frac{\tilde{\omega}_\beta(z)}{\sqrt{\tilde{\omega}_\beta^2(z) - \tilde{\phi}_\beta^2(z)}} + \mathrm{i}\Gamma_{\alpha\beta}(\omega) \frac{\tilde{\omega}_\beta(\omega)}{\sqrt{\tilde{\omega}_\beta^2(\omega) - \tilde{\phi}_\beta^2(\omega)}} \right\}, \tag{4}$$

[6] We would like to note that the considered transition occurs without the intermediate time-reversal symmetry breaking state which may exist at temperatures much lower than T_c at the surfaces of clean d-wave superconductors as predicted by Fogelstrom *et al* [12] and the surfaces of clean $s_{\pm}$ superconductors as recently proposed by Bobkov and Bobkova [12].

$$\tilde{\phi}_\alpha(\omega) = \sum_{\beta=a,b} \left\{ \int_{-\infty}^{\infty} \mathrm{d}z K^{\tilde{\phi}}_{\alpha\beta}(z,\omega) \mathrm{Re} \frac{\tilde{\phi}_\beta(z)}{\sqrt{\tilde{\omega}^2_\beta(z) - \tilde{\phi}^2_\beta(z)}} + \mathrm{i}\Gamma_{\alpha\beta}(\omega) \frac{\tilde{\phi}_\beta(\omega)}{\sqrt{\tilde{\omega}^2_\beta(\omega) - \tilde{\phi}^2_\beta(\omega)}} \right\}, \tag{5}$$

where the first terms on the right-hand side of the equations describe fermion–boson interaction, whereas the second terms stand for scattering of fermionic quasiparticles on impurities. The kernels $K^{\tilde{\phi},\tilde{\omega}}_{\alpha\beta}(z,\omega)$ of the fermion–boson interaction have the standard form [14]

$$K^{\tilde{\phi},\tilde{\omega}}_{\alpha\beta}(z,\omega) = \int_{-\infty}^{\infty} \mathrm{d}\Omega \frac{\lambda^{\tilde{\phi},\tilde{\omega}}_{\alpha\beta} B(\Omega)}{2} \times \left[\frac{\tanh\frac{z}{2T} + \coth\frac{\Omega}{2T}}{z + \Omega - \omega - \mathrm{i}\delta} \right]. \tag{6}$$

For simplicity, we use the same normalized spectral function of electron–boson interaction $B(\Omega)$ obtained for spin fluctuations in inelastic neutron scattering experiments [18] for all the channels. It is presented in the inset of figure 2. The maximum of the spectra is $\Omega_{sf} = 18\,\mathrm{meV}$ [7]. The matrix elements $\lambda^{\tilde{\phi}}_{\alpha\beta}$ are positive for attractive interactions and negative for repulsive ones. The symmetry of the order parameter in the clean case is determined solely by the off-diagonal matrix elements. The case $\mathrm{sign}\,\lambda^{\tilde{\phi}}_{ab} = \mathrm{sign}\,\lambda^{\tilde{\phi}}_{ba} > 0$ corresponds to s_{++} superconductivity and $\mathrm{sign}\,\lambda^{\tilde{\phi}}_{ab} = \mathrm{sign}\,\lambda^{\tilde{\phi}}_{ba} < 0$ to $s_{\pm}$. The matrix elements $\lambda^{\tilde{\omega}}_{\alpha\beta}$ have to be positive and are chosen $\lambda^{\tilde{\omega}}_{\alpha\beta} = |\lambda^{\tilde{\phi}}_{\alpha\beta}|$. For further model calculations we use the same matrix $\lambda^{\tilde{\phi}}_{aa} = 3$, $\lambda^{\tilde{\phi}}_{bb} = 0.5$, $\lambda^{\tilde{\phi}}_{ab} = -0.2$, $\lambda^{\tilde{\phi}}_{ba} = -0.1$ for the $s_{\pm}$-case and $\lambda^{\tilde{\phi}}_{aa} = 3$, $\lambda^{\tilde{\phi}}_{bb} = 0.5$, $\lambda^{\tilde{\phi}}_{ab} = 0.2$, $\lambda^{\tilde{\phi}}_{ba} = 0.1$ for the s_{++}-case (see [5, 7, 9]). The corresponding ratio of the densities of states is $N_a/N_b = 0.5$.

In the general case, $\Gamma_{\alpha\beta}(\omega)$ can be written in the following form:

$$\Gamma_{\alpha\beta}(\omega) = \gamma^{\mathrm{N}}_{\alpha\beta} I(\omega), \tag{7}$$

where the $\gamma^{\mathrm{N}}_{\alpha\beta}$ are inter- and intraband impurity scattering rates in the normal state. The dynamical part $I(\omega) = 1$ in the Born approximation (see the appendix). Beyond the Born approximation it reads

$$I(\omega) = \frac{1}{1 - 2\zeta C_{ab}(\omega)}, \tag{8}$$

where $C_{ab}(\omega)$ is the *coherence factor*:

$$C_{ab}(\omega) = 1 - \frac{\tilde{\omega}_a\tilde{\omega}_b - \tilde{\phi}_a\tilde{\phi}_b}{\sqrt{\tilde{\omega}^2_a - \tilde{\phi}^2_a}\sqrt{\tilde{\omega}^2_b - \tilde{\phi}^2_b}}. \tag{9}$$

Note that in the normal state, $C_{ab}(\omega) = 0$ and $I(\omega) = 1$.

The dimensionless constant ζ is related to the interband impurity scattering rate in the normal state γ^{N}_{ab} as

$$\gamma^{\mathrm{N}}_{ab} = \frac{n_{\mathrm{imp}}}{\pi N_a}\zeta. \tag{10}$$

The dependence of $\gamma^{\mathrm{N}}_{\alpha,\beta}$ and ζ on the scattering potential is shown in the appendix.

3. Quasiparticle properties

3.1. Density of states in superconductive state

Interband scattering is expected to modify the gap functions and the tunneling DOS in the superconducting state in a multiband superconductor. In the weak coupling regime the impurity effects have been discussed in [19] within the Born limit and extended in [20] to the strong coupling case. In the following, we will calculate the gap functions, and the superconducting DOS by solving the nonlinear Eliashberg equations in the $s_{\pm}$ and s_{++} superconductors for various values of the interband nonmagnetic scattering rate, going beyond the Born approximation.

The total DOS in the superconducting state is given by the following expression:

$$N(\omega) = \sum_{\alpha} N_{\alpha}(0) \mathrm{Re} \frac{\omega}{\sqrt{\omega^2 - \Delta_{\alpha}^2(\omega + \mathrm{i}\delta)}}, \tag{11}$$

where we have introduced the *complex gap functions*:

$$\Delta_{\alpha}(\omega + \mathrm{i}\delta) \equiv \omega \tilde{\phi}_{\alpha}(\omega + \mathrm{i}\delta)/\tilde{\omega}_{\alpha}(\omega + \mathrm{i}\delta) = \mathrm{Re}\, \Delta_{\alpha}(\omega) + \mathrm{i}\, \mathrm{Im}\, \Delta_{\alpha}(\omega). \tag{12}$$

The solution for $\Delta_{\alpha}(\omega)$ allows calculation of the current–voltage characteristic $I(V)$ and the *tunnelling conductance* $G_{\mathrm{NS}}(V) = \mathrm{d}I_{\mathrm{NS}}/\mathrm{d}V$ in the superconducting state of the NIS tunneling junction.

In contrast to a single-band case, where DOS does not depend on *nonmagnetic* impurities, in the multiband case $\Delta_{\alpha}(\omega + \mathrm{i}\delta)$ and DOS are strongly dependent on interband impurity scattering.

Figure 1 shows the calculated gap functions $\mathrm{Re}\, \Delta_{\alpha}(\omega)$ for the bands a and b for different interband impurity scattering rates. One sees in both the $s_{\pm}$ and s_{++} cases a strong nonmonotonic frequency dependence of the gap function with the maxima of the absolute values around $250\,\mathrm{cm}^{-1}$ for a-band and $140\,\mathrm{cm}^{-1}$ for b-band, originating from the strong electron–boson coupling. Furthermore, the effects of impurity scattering are visible as an additional structure at low energies comparable to the interband scattering rate Γ_a. The most spectacular effect is the impurity-induced sign change of $\mathrm{Re}\, \Delta_b(\omega)$ at low energies comparable to the bulk gap in b-band, in accord with the scenario of $s_{\pm} \to s_{++}$ transition discussed in [9] in Matsubara representation. At the transition point, the gap function at small frequencies vanishes, leading to the anomalies of DOS, ARPES and optical conductivity which are discussed below.

Figure 2 shows a comparison of DOS in $s_{\pm}$ and s_{++} states for different magnitudes of the interband scattering rate Γ_a at low temperatures T. In the clean limit, one sees two different excitation gaps for the two bands. In accord with earlier calculations for s_{++} superconductors [20], the interband impurity scattering mixes the pairs in the two bands, so that the states appear in the a-band at the energy range of the b-band gap. These states are gradually filled in with increasing scattering rate. At the same time the minimal b-band gap in the DOS rises due to increased mixing to the a-band with strong electron–boson coupling. In the $s_{\pm}$ superconductor, the modification of low-energy DOS with interband impurity scattering is completely different. Due to sign change of $\mathrm{Re}\, \Delta(\omega)$ in the b-band, a gapless region exists in a range of values of scattering parameter Γ around $35\,\mathrm{cm}^{-1}$, as clearly seen in the left panel of figure 2. Such gapless behavior manifests itself in optical properties of $s_{\pm}$ superconductors, as will be demonstrated below.

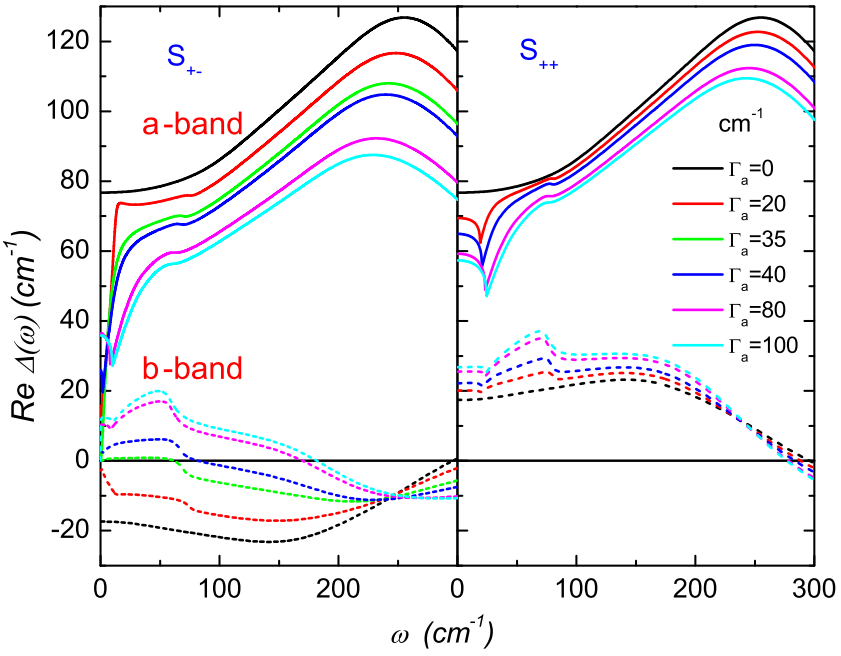

Figure 1. Superconducting gap functions for bands a and b at various interband impurity scattering rates in $s_{\pm}$ and s_{++} models. The parameters are $\zeta \approx 0.2$, $\gamma_{bb}^{\mathrm{N}} = 2\gamma_{aa}^{\mathrm{N}} = \gamma_{ab}^{\mathrm{N}} = 2\gamma_{ba}^{\mathrm{N}} \approx 0.4\Gamma_a$. They correspond to scattering strength $\sigma = 0.5$. The relation between σ and Γ_a to the scattering potential is given in the appendix.

3.2. Angle-resolved photoemission spectroscopy and the self-energy

ARPES probes the photoemission current $I(\mathbf{k}, \omega)$, which in the simple sudden approximation can be calculated as

$$I(\mathbf{k}, \omega) = \sum_{\alpha} |M_{\alpha}(\mathbf{k}, \omega)|^2 f(\omega) A_{\alpha}(\mathbf{k}, \omega).$$

Here $M(\mathbf{k}, \omega)$ is the dipole matrix element that depends on the initial and final electronic states, incident photon energy and polarization, $f(\omega)$ is the Fermi distribution function and

$$A_{\alpha}(\mathbf{k}, \omega) = -\frac{1}{2\pi}\mathrm{Tr}\left\{\mathrm{Im}\,\hat{G}_{\alpha}(\mathbf{k}, \omega)\hat{\tau}_0\right\}$$

$$= -\frac{1}{\pi}\mathrm{Im}\frac{\tilde{\omega}_{\alpha}(\omega)}{\tilde{\omega}_{\alpha}^2(\omega) - \xi_{\alpha}^2(\mathbf{k}) - \tilde{\phi}_{\alpha}^2(\omega)} \tag{13}$$

is a single-particle response function.

In the weak coupling limit, the contribution of the electron–boson interaction to self-energy $\Sigma_{\alpha 0}(\mathbf{k}, \omega)$ (see the first terms on lhs of equations (4) and (5)) vanishes. It means that in the model with isotropic self-energy $\Sigma_{\alpha 0}^{\mathrm{e-b}}(\omega) \to 0$, $\Sigma_{\alpha 1}^{\mathrm{e-b}}(\omega) \to \Delta_{\alpha}(\omega)$. Then the single-particle spectral function takes the form

$$A_{\alpha}(\mathbf{k}, \omega) = \frac{1}{\pi}\mathrm{Im}\frac{\omega\left[1 + \mathrm{i}\sum_{\beta=a,b}\Gamma_{\alpha\beta}/\sqrt{\omega^2 - \Delta_{\beta}^2(\omega)}\right]}{D_{\alpha}}$$

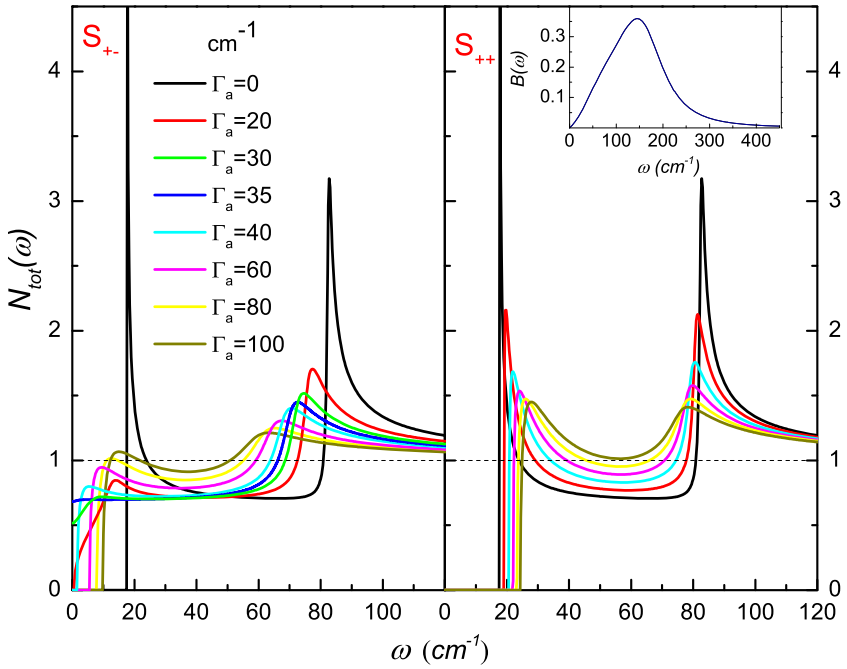

Figure 2. Total DOS for various impurity scattering rates in $s_{\pm}$ and s_{++} models at low temperature $T \ll T_{c0}$. The parameters are the same as in figure 1. The inset shows the electron–boson interaction function $B(\Omega)$.

with

$$D_\alpha = \xi_\alpha^2(\mathbf{k}) + [\Delta_\alpha^2(\omega) - \omega^2]\left(1 + \mathrm{i}\sum_{\beta=a,b}\Gamma_{\alpha\beta}/\sqrt{\omega^2 - \Delta_\beta^2(\omega)}\right)^2.$$

In the gapped regime $A_\alpha(\mathbf{k}, \omega)$ vanishes below Δ_β but in the gapless one for b-band it is the same as in the normal state:

$$A_b(\mathbf{k}, \omega) = \frac{1}{\pi}\mathrm{Im}\frac{\omega\left[1 + \mathrm{i}\sum_{\beta=a,b}\Gamma_{b\beta}/|\omega|\right]}{\xi_b^2(\mathbf{k}) - \omega^2\left(1 + \mathrm{i}\sum_{\beta=a,b}\Gamma_{b\beta}/|\omega|\right)^2}.$$

The quasiparticle spectral function $A_b(\mathbf{k}, \omega)$ given by equation (13) for b-band is shown in figure 3. In this case the behavior of $A_b(\mathbf{k}, \omega)$ at small ω and $\xi(\mathbf{k})$ reflects the existence of a well-defined energy gap. In contrast to that, the function $A_b(\mathbf{k}, \omega)$ in the regime of $s_{\pm} \to s_{++}$ transition shows no gap, as seen from figure 4. With further increase of scattering rate Γ_a, when s_{++} state is realized, in the b-band an energy gap appears again. Therefore, ARPES measurements at various impurity concentrations may provide a useful tool to distinguish the underlying pairing symmetry of the superconducting state in pnictides.

4. Optical conductivity

The optical conductivity in the London (local, $\mathbf{q} \equiv 0$) limit in the a–b plane is given by

$$\sigma(\omega) = \sum_\alpha \omega_{\mathrm{pl},\alpha}^2 \Pi_\alpha(\omega)/4\pi\mathrm{i}\omega, \tag{14}$$

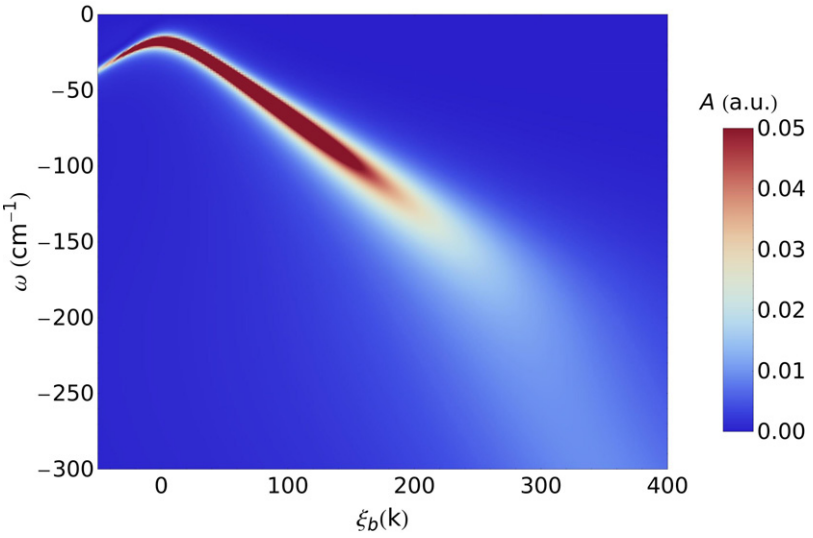

Figure 3. The quasiparticle spectral function $A_b(\mathbf{k}, \omega)$ for b-band with a small gap in the clean limit. The parameters are the same as in figure 1.

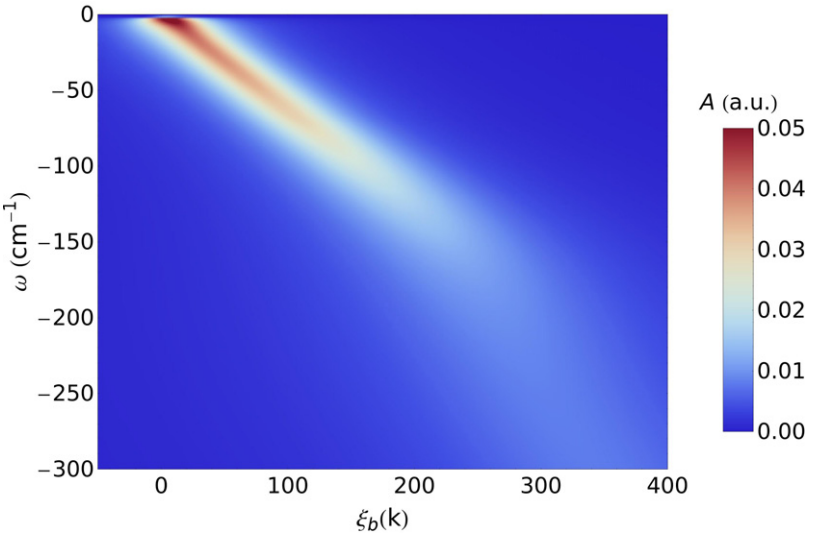

Figure 4. The quasiparticle spectral function $A_b(\mathbf{k}, \omega)$ for b-band with a small gap in the gapless regime ($\Gamma_a = 40\,\mathrm{cm}^{-1}$). The parameters are the same as in figure 1.

where $\Pi_\alpha(\omega)$ is an analytical continuation to the real frequency axis of the polarization operator (see, e.g., [21–25])

$$\Pi_\alpha(\omega) = \left\{ i\pi T \sum_n \Pi_\alpha(\omega'_n, \nu_m) \right\}_{i\nu_m \Longrightarrow \omega + i0^+},$$

$\alpha = a, b$ is the band index.

$$\Pi_\alpha(\omega) = \int \mathrm{d}\omega' \left\{ \frac{\tanh\left(\frac{\omega_-}{2T}\right)}{D^{\mathrm{R}}} \left[1 - \frac{\tilde{\omega}_-^{\mathrm{R}}\tilde{\omega}_+^{\mathrm{R}} + \tilde{\phi}_-^{\mathrm{R}}\tilde{\phi}_+^{\mathrm{R}}}{Q_-^{\mathrm{R}} Q_+^{\mathrm{R}}}\right] - \frac{\tanh\left(\frac{\omega_+}{2T}\right)}{D^{A}} \left[1 - \frac{\tilde{\omega}_-^{\mathrm{A}}\tilde{\omega}_+^{\mathrm{A}} + \tilde{\phi}_-^{\mathrm{A}}\tilde{\phi}_+^{\mathrm{A}}}{Q_-^{\mathrm{A}} Q_+^{\mathrm{A}}}\right] \right.$$
$$\left. - \frac{\tanh\left(\frac{\omega_+}{2T}\right) - \tanh\left(\frac{\omega_-}{2T}\right)}{D^{a}} \left[1 - \frac{\tilde{\omega}_-^{\mathrm{A}}\tilde{\omega}_+^{\mathrm{R}} + \tilde{\phi}_-^{\mathrm{A}}\tilde{\phi}_+^{\mathrm{R}}}{Q_-^{\mathrm{A}} Q_+^{\mathrm{R}}}\right] \right\}, \tag{15}$$

where

$$Q_\pm^{\mathrm{R,A}} = \sqrt{(\tilde{\omega}_\pm^{\mathrm{R,A}})^2 - (\tilde{\phi}_\pm^{\mathrm{R,A}})^2},$$

$$D^{\mathrm{R,A}} = \sqrt{(\tilde{\omega}_+^{\mathrm{R,A}})^2 - (\tilde{\phi}_+^{\mathrm{R,A}})^2} + \sqrt{(\tilde{\omega}_-^{\mathrm{R,A}})^2 - (\tilde{\phi}_-^{\mathrm{R,A}})^2}$$

and

$$D^{a} = \sqrt{(\tilde{\omega}_+^{\mathrm{R}})^2 - (\tilde{\phi}_+^{\mathrm{R}})^2} - \sqrt{(\tilde{\omega}_-^{\mathrm{A}})^2 - (\tilde{\phi}_-^{\mathrm{A}})^2},$$

$\omega_\pm = \omega' \pm \omega/2$, and the index R (A) corresponds to the retarded (advanced) branch of the complex function $F^{\mathrm{R(A)}} = \mathrm{Re}\, F \pm \mathrm{i}\, \mathrm{Im}\, F$ (the band index α is omitted).

In the normal state the conductivity is

$$\sigma_\alpha^{\mathrm{N}}(\omega) = \frac{\omega_{\mathrm{pl}}^2}{8\mathrm{i}\pi\omega} \int_{-\infty}^{\infty} \mathrm{d}z \frac{\tanh((z+\omega)/2T) - \tanh(z/2T)}{\tilde{\omega}_\alpha(z+\omega) - \tilde{\omega}_\alpha(z)}.$$

If the dominant contribution to the quasiparticle damping comes from the impurity scattering, it reduces to the Drude formula

$$\sigma_a(\omega, T) = \frac{\omega_{\mathrm{pl}}^2}{4\pi} \frac{1}{\gamma_a^{\mathrm{opt}} - \mathrm{i}\omega}$$

with $\gamma_a^{\mathrm{opt}} = \gamma_{ab} + \gamma_{aa}$.

In figure 5 we demonstrate the impact of disorder on the optical conductivity $\mathrm{Re}\,\sigma(\omega)$. In the clean limit one sees that $\mathrm{Re}\,\sigma_\alpha(\omega) = 0$ for $\omega < 2\Delta_\alpha$. With an increase of the impurity scattering rate the region $\mathrm{Re}\,\sigma_b(\omega) = 0$ for the band b decreases and the peak above $2\Delta_b$ becomes sharper. It is clearly seen that in the vicinity of the transition from the $s_\pm$ to s_{++} state ($\Gamma_a \sim 35\,\mathrm{cm}^{-1}$), the conventional Drude-response characteristic in the weak for a normal metal state is realized. The origin of this effect is the gapless nature of superconductivity near the impurity-induced $s_\pm \to s_{++}$ transition. With a further increase of the impurity scattering rate, the optical conductivity recovers gapped-like behavior, but with smaller gap. It is strikingly different from the behavior of superconductors with s_{++} order parameter (figure 5(b)), where the values of two gaps tend to merge at the limit of infinite impurity scattering rate. This reentrant behavior of optical conductivity with concentration of nonmagnetic impurities may serve as an unambiguous indication of the $s_\pm$ order parameter symmetry.

Another important characteristic of the superconducting state is the real part of the electromagnetic kernel (polarization operator) which is related to the imaginary part of optical conductivity $\mathrm{Im}\,\sigma(\omega)$ (see equation (14)). Figure 6 shows the frequency dependence of $\mathrm{Re}\,\Pi(\omega)$ for $s_\pm$ and s_{++} models for various interband scattering rates. One can see that in the s_{++} case dips

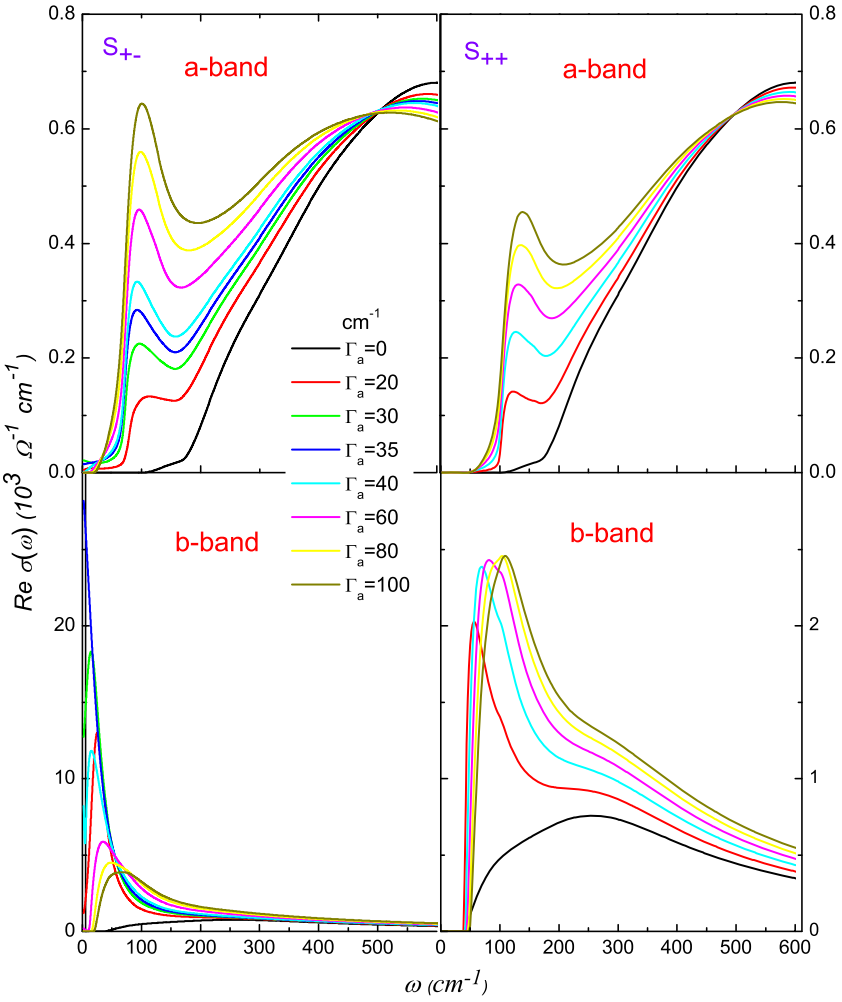

Figure 5. Real part of the optical conductivity $\mathrm{Re}\,\sigma(\omega)$ for various values of Γ_a. The parameters are the same as in figure 1 and $\omega_{\mathrm{pl}1} = \omega_{\mathrm{pl}2} = 1$ eV.

at $\omega = 2\Delta_\alpha(\omega)$ occur for nonzero scattering, in accord with previous calculations performed for single-band superconductors [26]. Further, an interesting peculiarity is seen in the response of the b-band in the $s_\pm$ state: the dip position is a nonmonotonic function of interband scattering rate and the dip vanishes completely in the gapless regime corresponding to the $s_\pm \to s_{++}$ transition.

The magnetic field penetration depth $\lambda_{\mathrm{L}}(T)$ in the local (London) limit in the a–b plane is related to $\mathrm{Im}\,\sigma(\omega)$ in the zero frequency limit [27]

$$1/\lambda_{\mathrm{L}}^2(T) = \sum_{\alpha=a,b} \lim_{\omega\to 0} 4\pi\omega\,\mathrm{Im}\,\sigma_\alpha(\omega, \mathbf{q}=0, T)/c^2, \tag{16}$$

where c is the velocity of light. If we neglect strong-coupling effects (or, more generally, Fermi-liquid effects), then for a clean uniform superconductor at $T = 0$ we have the relation $\lambda_{\mathrm{L}} = c/\omega_{\mathrm{pl}}$, where $\omega_{\mathrm{pl},\alpha} = \sqrt{8\pi e^2\langle N_\alpha(0) v_{F\alpha} v_{F\alpha}\rangle}$ is the plasma frequency in different bands.

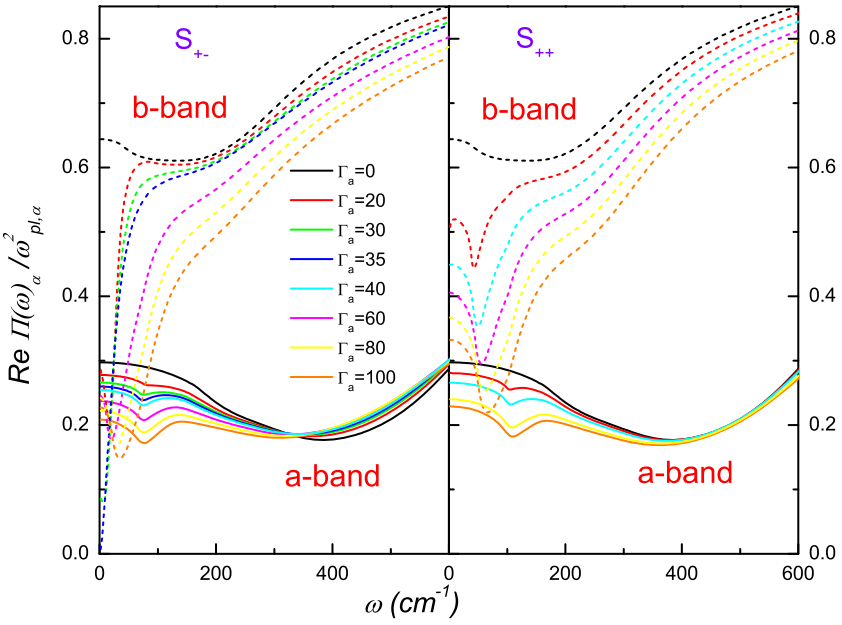

Figure 6. Real part of the polarization operator for various values of Γ_a. The parameters are the same as in figure 1.

Partial contributions to the magnetic field penetration depth can be written as

$$1/\lambda_{\mathrm{L}}^2(T) = \mathrm{Re} \sum_{\alpha=a,b} \frac{\omega_{\mathrm{pl},\alpha}^2}{c^2} \int_{\omega_{\mathrm{g}}(T)-0}^{\infty} \frac{\mathrm{d}\omega \tanh(\omega/2T)}{Z_\alpha(\omega,T)\sqrt{\omega^2-\Delta_\alpha^2(\omega,T)}} \frac{\Delta_\alpha^2(\omega,T)}{\left[\Delta_\alpha^2(\omega,T)-\omega^2\right]}. \tag{17}$$

Here the points $\omega_{\mathrm{g}}(T)$ are determined by the condition for the DOS in the band

$$\mathrm{Re}\, N(\omega < \omega_{\mathrm{g}}(T)) = 0.$$

For superconductors with gap nodes as well as for $T > 0$: $\omega_{\mathrm{g}}(T) \equiv 0$ (see [16]).

Peculiarities of the penetration depth in the crossover regime from $s_\pm$ to s_{++} state have been discussed earlier [9].

5. Conclusions

We have studied the effects of the impurity-induced $s_\pm \to s_{++}$ transition in the DOS, the single-particle response function and optical conductivity in multiband superconductors with $s_\pm$ symmetry of the order parameter. It has been shown that a smaller gap vanishes in the vicinity of this transition, leading to the gapless nature of photoemission and tunneling spectra. In the optical response, the $s_\pm \to s_{++}$ transition leads to 'restoring' of the 'Drude'-like frequency dependence of $\mathrm{Re}\,\sigma(\omega)$. We also found interesting anomalies in the real part of the polarization operator, with reentrant behavior of the dip-like structure at $\omega = 2\Delta_\alpha(\omega)$ as a function of interband scattering rate. This effect leads to nonmonotonic behavior in the magnetic field penetration depth as a function of the impurity concentration.

We wish to stress that a systematic study of the impact of disorder on the single-particle response function and optical conductivity may provide information about the underlying symmetry of the superconductive order parameter.

Acknowledgments

The authors are grateful to P Hirschfeld, M M Korshunov, A Charnukha, A V Boris and B Keimer for useful discussions. This work was partially supported by the DFG Priority Programme SPP1458 (DVE), the Dutch FOM and the EU–Japan program IRON SEA (AAG).

Appendix

The impurity part of the self-energy is obtained by analytic continuation of the corresponding self-energy on Matsubara frequencies $\hat{\Sigma}^{\rm imp}_{\alpha\beta}(\mathrm{i}\omega_n) = \Sigma^{\rm imp(0)}_{\alpha\beta}(\mathrm{i}\omega_n)\hat{\tau}_0 + \Sigma^{\rm imp(3)}_{\alpha\beta}(\mathrm{i}\omega_n)\hat{\tau}_3$ derived in [9]. The last is taken in the T-matrix approximation:

$$\hat{\Sigma}^{\rm imp}(\omega_n) = n_{\rm imp}\hat{\mathbf{U}} + \hat{\mathbf{U}}\hat{\mathbf{g}}(\omega_n)\hat{\Sigma}^{\rm imp}(\mathrm{i}\omega_n), \tag{A.1}$$

where $\hat{\mathbf{U}} = \mathbf{U}\otimes\hat{\tau}_3$ and $n_{\rm imp}$ is the impurity concentration and the scattering potential:

$$\mathbf{U} = \begin{pmatrix} U_{aa} & U_{ba} \\ U_{ab} & U_{bb} \end{pmatrix}.$$

The quasiclassical Nambu Green's functions on Matsubara frequencies are:

$$g_{0\alpha} = -\frac{\mathrm{i}\pi N_\alpha \tilde{\omega}_{\alpha n}}{\sqrt{\tilde{\omega}^2_{\alpha n} + \tilde{\phi}^2_{\alpha n}}}, \quad g_{1\alpha} = -\frac{\pi N_\alpha \tilde{\phi}_{\alpha n}}{\sqrt{\tilde{\omega}^2_{\alpha n} + \tilde{\phi}^2_{\alpha n}}}. \tag{A.2}$$

Solutions of equations (A.1) for $\Sigma^{\rm imp(0)}_{aa}$ and $\Sigma^{\rm imp(1)}_{aa}$ are

$$\Sigma^{\rm imp(0)}_{aa} = n_{\rm imp}\frac{U^2_{aa} - (\det\mathbf{U})^2\left(g^2_{0b} - g^2_{1b}\right)}{D(\omega_n)}\, g_{0b} + n_{\rm imp}\frac{U_{ab}U_{ba}}{D(\omega_n)}\, g_{0b}, \tag{A.3}$$

$$\Sigma^{\rm imp(1)}_{aa} = -n_{\rm imp}\frac{U^2_{aa} - (\det\mathbf{U})^2\left(g^2_{0b} - g^2_{1b}\right)}{D(\omega_n)}\, g_{1a} - n_{\rm imp}\frac{U_{ab}U_{ba}}{D(\omega_n)}\, g_{1b}, \tag{A.4}$$

where

$$\begin{aligned} D(\omega_n) = 1 &- \left(g^2_{0a} - g^2_{1a}\right)U^2_{aa} - \left(g^2_{0b} - g^2_{1b}\right)U^2_{bb} + \left(g^2_{0a} - g^2_{1a}\right)\left(g^2_{0b} - g^2_{1b}\right)(\det\mathbf{U})^2 \\ &- 2U_{ab}U_{ba}\left(g_{0a}g_{0b} - g_{1a}g_{1b}\right). \end{aligned} \tag{A.5}$$

The analytical continuation on the real axis leads to the following expression:

$$\hat{\boldsymbol{\Sigma}}^{\rm imp(0)}(\omega) = \sum_{\beta=a,b} \mathrm{i}\Gamma_{\alpha\beta}(\omega)\frac{\tilde{\omega}_\beta(\omega)}{\sqrt{\tilde{\omega}^2_\beta(\omega) - \tilde{\phi}^2_\beta(\omega)}}$$

and

$$\hat{\boldsymbol{\Sigma}}^{\rm imp(1)}(\omega) = \sum_{\beta=a,b} \mathrm{i}\Gamma_{\alpha\beta}(\omega)\frac{\tilde{\phi}_\beta(\omega)}{\sqrt{\tilde{\omega}^2_\beta(\omega) - \tilde{\phi}^2_\beta(\omega)}}$$

with $\Gamma_{\alpha\beta}(\omega)$ given by equation (7).

The dimensionless constant ζ is convenient to express in terms of dimensionless scattering potentials $\bar{u}_{\alpha\beta} = \pi U_{\alpha\beta} N_\beta$ and $\bar{d} = \bar{u}_{aa}\bar{u}_{bb} - \bar{u}_{ab}\bar{u}_{ba}$. Then it has the following compact form:

$$\zeta = \frac{\bar{u}_{ab}\bar{u}_{ba}}{(\bar{d}-1)^2 + (\bar{u}_{aa}+\bar{u}_{bb})^2}. \tag{A.6}$$

The normal state impurity scattering rate reads

$$\gamma^{\mathrm{N}}_{\alpha\alpha} = \frac{n_{\mathrm{imp}}}{\pi N_\alpha} \frac{d^2 + \bar{u}^2_{\alpha\alpha}}{(\bar{d}-1)^2 + (\bar{u}_{aa}+\bar{u}_{bb})^2} \tag{A.7}$$

and for $\alpha \neq \beta$

$$\gamma^{\mathrm{N}}_{\alpha\beta} = \frac{n_{\mathrm{imp}}}{\pi N_\alpha} \frac{\bar{u}_{ab}\bar{u}_{ba}}{(\bar{d}-1)^2 + (\bar{u}_{aa}+\bar{u}_{bb})^2}. \tag{A.8}$$

The Born approximation corresponds to $\bar{u}_{\alpha\beta} \ll 1$. Then up to quadratic terms in $\bar{u}$ one obtains

$$\Gamma_{aa}(\omega) \approx \gamma^{\mathrm{N}}_{aa} \approx n_{\mathrm{imp}} \pi N_a U^2_{aa}$$

and

$$\Gamma_{ab}(\omega) \approx \gamma^{\mathrm{N}}_{ab} \approx n_{\mathrm{imp}} \pi N_b U^2_{ab}.$$

It is worth introducing the parameters $\sigma = \bar{u}_{ab}\bar{u}_{ba}/(1+\bar{u}_{ab}\bar{u}_{ba})$ and $\Gamma_a = n_{\mathrm{imp}} \frac{\sigma}{\pi N_a} = n_{\mathrm{imp}} \pi N_b U_{ab} U_{ba} (1-\sigma)$. The parameter σ is used as an indicator of the strength of the impurity scattering. In the Born approximation $\sigma \to 0$, while in the opposite unitary limit $\sigma \to 1$.

References

[1] Kamihara Y, Watanabe T, Hirano M and Hosono H 2008 *J. Am. Chem. Soc.* **130** 3296

[2] See e.g. 2008 Superconductivity in iron-pnictides *Physica* C **469** 313–674
Hirschfeld P J, Korshunov M M and Mazin I I 2011 *Rep. Prog. Phys.* **74** 124508

[3] Mazin I I, Singh D J, Johannes M D and Du M H 2008 *Phys. Rev. Lett.* **101** 057003

[4] Evtushinsky D V *et al* 2012 arXiv:1204.2432v1
Huang Y-B, Richard P, Wang X-P, Qian T and Ding H 2012 arXiv:1208.4717
Donghui L, Vishik I M, Ming Yi, Chen Y, Moore R G and Shen Z-X 2012 *Annu. Rev. Condens. Matter Phys.* **3** 129

[5] Popovich P, Boris A V, Dolgov O V, Golubov A A, Sun D L, Lin C T, Kremer R K and Keimer B 2010 *Phys. Rev. Lett.* **105** 027003

[6] Hardy F *et al* 2010 *Europhys. Lett.* **91** 47008

[7] Charnukha A, Dolgov O V, Golubov A A, Matiks Y, Sun D L, Lin C T, Keimer B and Boris A V 2011 *Phys. Rev.* B **84** 174511

[8] Kontani H and Onari S 2010 *Phys. Rev. Lett.* **104** 157001
Senga Y and Kontani H 2008 *J. Phys. Soc. Japan* **77** 113710
Onari S and Kontani H 2009 *Phys. Rev. Lett.* **103** 177001

[9] Efremov D V, Korshunov M M, Dolgov O V, Golubov A A and Hirschfeld P J 2011 *Phys. Rev.* B **84** 180512

[10] Golubov A A and Mazin I I 1997 *Phys. Rev.* B **55** 15146
Golubov A A and Mazin I I 1995 *Physica* C **243** 153

[11] Kulić M L and Dolgov O V 1999 *Phys. Rev.* B **60** 13062
Ohashi Y 2004 *Physica* C **412–414** 41

[12] Fogelstrom M, Rainer D and Sauls J A 1997 *Phys. Rev. Lett.* **79** 281
Bobkov A M and Bobkova I V 2011 *Phys. Rev.* B **84** 134527

[13] Allen P B and Mitrović B 1982 *Solid State Phys.* **37** 3

[14] Scalapino D J 1969 *Superconductivity* ed R D Parks (New York: Marcel Dekker) chapter 10, p 449
[15] Parker D, Dolgov O V, Korshunov M M, Golubov A A and Mazin I I 2008 *Phys. Rev.* B **78** 134524
[16] Maksimov E G and Khomskii D I 1982 *High Temperature Superconductivity* ed V L Ginzburg and D Kirzhnitz (New York: Consultant Bureau) chapter 4
[17] Vonsovskij S V, Izjumov Yu A and Kurmaev E Z 1982 *Superconductivity of Transition Metals: Their Alloys and Compounds* (Berlin: Springer)
[18] Inosov D S *et al* 2009 *Nature Phys.* **6** 178
[19] Schopohl N and Scharnberg K 1977 *Solid State Commun.* **22** 371
[20] Dolgov O V, Kremer R K, Kortus J, Golubov A A and Shulga S V 2005 *Phys. Rev.* B **72** 024504
[21] Nam S B 1967 *Phys. Rev.* **156** 470
[22] Lee W, Rainer D and Zimmermann W 1988 *Physica* C **159** 535
[23] Dolgov O V, Golubov A A and Shulga S V 1990 *Phys. Lett.* A **147** 317
[24] Akis R and Carbotte J P 1991 *Solid State Commun.* **79** 577
[25] Marsiglio F 1991 *Phys. Rev.* B **44** 5373
[26] Marsiglio F, Carbotte J P, Puchkov A and Timusk T 1996 *Phys. Rev.* B **53** 9433
[27] Golubov A A, Brinkman A, Dolgov O V, Kortus J and Jepsen O 2002 *Phys. Rev.* B **66** 054524
Kogan V G, Martin C and Prozorov R 2009 *Phys. Rev.* B **80** 014507